Journal of Nanoparticle Research (2006) 8: 489–496
DOI 10.1007/s11051-005-9011-3

Iron/iron oxide core-shell nanoclusters for biomedical applications

You Qiang*, Jiji Antony, Amit Sharma, Joseph Nutting, Daniel Sikes and Daniel Meyer
*Department of Physics, University of Idaho, Moscow, ID, 83844–0903, USA; *Author for correspondence (Tel.: +1-208-885-7558; E-mail: youqiang@uidaho.edu)*

Received 30 June 2005; accepted in revised form 20 July 2005

Key words: magnetic nanoparticles, nanocluster, core-shell structure, biomagnetic sensor, medicine

Abstract

Biocompatible magnetic nanoparticles have been found promising in several biomedical applications for tagging, imaging, sensing and separation in recent years. Most magnetic particles or beads currently used in biomedical applications are based on ferromagnetic iron oxides with very low specific magnetic moments of about 20–30 emu/g. Here we report a new approach to synthesize monodispersed core-shell nanostructured clusters with high specific magnetic moments above 200 emu/g. Iron nanoclusters with monodispersive size of diameters from 2 nm to 100 nm are produced by our newly developed nanocluster source and go to a deposition chamber, where a chemical reaction starts, and the nanoclusters are coated with iron oxides. HRTEM Images show the coatings are very uniform and stable. The core-shell nanoclusters are superparamagnetic at room temperature for sizes less than 15 nm, and then become ferromagnetic when the cluster size increases. The specific magnetic moment of core-shell nanoclusters is size dependent, and increases rapidly from about 80 emu/g at the cluster size of around 3 nm to over 200 emu/g up to the size of 100 nm. The use of high magnetic moment nanoclusters for biomedical applications could dramatically enhance the contrast for MRI, reduce the concentration of magnetic particle needs for cell separation, or make drug delivery possible with much lower magnetic field gradients

Introduction

Nanoclusters are ultrafine particles of nanometer dimensions located in the transition region between molecules and microscopic (micron-size) structures. Viewed as molecules, they are so large that they provide access to realms of quantum behavior that are not otherwise accessible; viewed as bulk materials, they are so small that they exhibit characteristics that are not observed in larger (even 100 nm) structures. It is in this size regime that many recent advances have been made in biology, physics, and chemistry (Whitesides, 1999; Brigger 2002; Cancer, 2004). Since their introduction in the mid-1970s, magnetic particles (submicro- and microspheres and ferrofluids) have been widely studied for their applications in various fields in biology and medicine such as magnetic targeting (drugs, genes, radio-pharmaceuticals), magnetic resonance imaging (MRI), diagnostics, immunoassays, RNA and DNA purification, cell separation and purification as well as hyperthermia generation (Hadjipanayis, 1994; Haefili, 1997; Andra, 1998). Nanotechnology is beginning to allow scientists,

engineers, and physicians to work at the cellular and molecular levels to produce major advances in the life sciences and healthcare.

We can classify biomedical applications of magnetic nanoparticles (MNPs) according to their application inside (*in vivo*) or outside (*in vitro*) the body. *In vivo* applications could be further separated in therapeutic (hyperthermia and drug-targeting) and diagnostic applications (nuclear magnetic resonance (NMR) imaging), while for *in vitro* applications the main use is in diagnostic (separation/selection and magnetorelaxometry).

Iron oxide particles such as magnetite (Fe_3O_4) or maghemite (γ-Fe_2O_3) are by far the most commonly employed for biomedical applications. Highly magnetic materials such as cobalt and nickel are toxic, susceptible to oxidation and hence are of little interest. Moreover, the main advantage of using particles of sizes smaller than 100 nm is their higher effective surface areas (easier attachment of ligands), lower sedimentation rates (high stability) and improved tissular diffusion (Portet, 2001). Therefore, for *in vivo* biomedical applications, MNPs must be made of a non-toxic and non-immunogenic material, with particle sizes small enough to remain in the circulation after injection and to pass through the capillary systems of organs and tissues avoiding vessel embolism. They must also have a high magnetization so that their movement in the blood can be controlled with a magnetic field and so that they can be immobilized close to the targeted pathologic tissue (Jordan, 2001).

For *in vitro* applications the size restrictions are not so severe as in *in vivo* applications. Therefore, composites consisting of superparamagnetic nanocrystals dispersed in submicron diamagnetic particles with long sedimentation times in the absence of a magnetic field can be used. The advantage of using diamagnetic matrixes is that the superparamagnetic composites can be easily provided with functionality.

For biomedical applications the use of particles that present superparamagnetic behavior at room temperature (no remanence along with a rapidly changing magnetic state) is preferred. Furthermore, applications in biology and medical diagnosis and therapy require the MNPs to be stable in water at neutral pH and physiological salinity.

In almost all applications the preparation method of the nanomaterials represents one of the most important challenges that will determine the particle size and shape, the size distribution, the surface chemistry of the particles and consequently their magnetic properties. Recently many attempts have been made to develop processes and techniques that would yield 'monodispersed colloids' consisting of uniform nanoparticles both in size and shape (Matijevic, 1993; Sugimoto, 2000). Monodispersed colloids have been exploited in fundamental research and as models in the quantitative assessment of properties that depend on the particle size and shape. In addition, it has become evident that the quality and reproducibility of commercial products can be more readily achieved by starting with well-defined MNPs of known properties.

MNPs such as Fe_3O_4 and Fe_2O_3, coated with compounds such as dextran or starch for biocompatibility, are now widely used (Zhao, 2002; Fritzsche, 2003; Hatch, 2001; Kim, 2003; Reich, 2003; Tada, 2003). Ferrite nanoparticles are biocompatible and easily synthesized, but the specific magnetic moment of ferromagnetic iron oxide particles is very low. Most MNPs used currently are based on ferromagnetic iron oxides with low specific magnetic moment of about 20–30 emu/g. Iron has a greater specific magnetization than either of these iron oxides. The problem is that pure metallic iron nanoparticles are highly sensitive to oxidation and dissolution through electrochemical reactions. If iron nanoparticles were passivated with a thin ion oxide- or Au-shell and retain the high magnetic moments of pure iron cores, they will dramatically enhance the contrast for MRI, reduce the concentration of magnetic particles needed for cell separation, or make drug delivery possible with much lower magnetic field gradients.

To realize this goal, we apply a new approach of our newly developed nanocluster deposition system to synthesize monodispersive, high specific magnetic moment core-shell nanostructured clusters.

Experiment

Figure 1 shows a photo and a schematic view of a newly developed nanocluster deposition apparatus, based on the earlier two generations of cluster deposition system built by Y. Qiang at the University of Freiburg, Germany, and the University

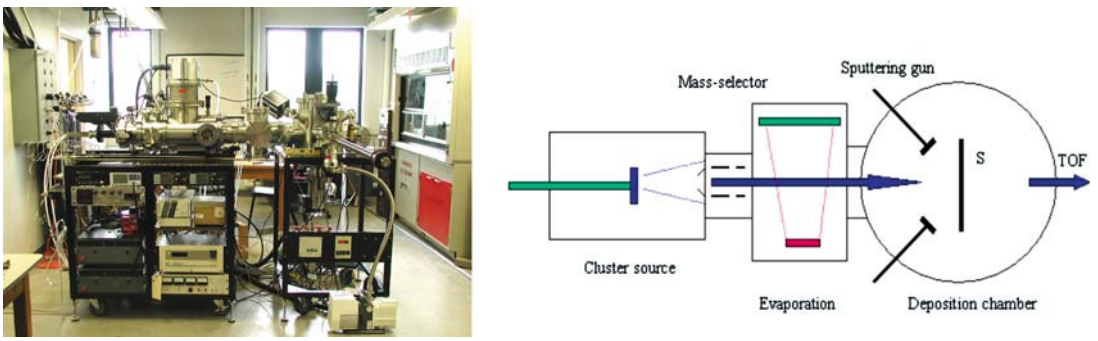

Figure 1. Nanocluster deposition system.

of Nebraska-Lincoln (Qiang, 1998, 2000, 2002, 2004; Meldrim, 2000; Sellmyer, 2002; Xu, 2003].

The system uses a combination of magnetron-sputtering and gas–aggregation techniques. The cluster beam deposition apparatus is mainly composed of three parts: a cluster source, an e-beam evaporation chamber and a deposition chamber. The sputtered Fe atoms from a high-pressure magnetron-sputtering gun are decelerated by collisions with Ar gas (the flow rate: 100–500 sccm) injected continuously into the cluster growth chamber, which is cooled by chilled water. The clusters formed in this chamber are ejected from a small nozzle by differential pumping and a part of the cluster beam is intercepted by a skimmer, and then deposited onto a sample holder in the deposition chamber. The mean size of clusters, from 1 to 100 nm, is easily varied by adjusting the aggregation distance, the sputter power, the pressure in the aggregation tube, and the ratio of He to Ar gas flow rate. The aggregation distance and the ratio of He to Ar gas flow rate are important parameters for getting a very high intensity (>5 Å/s), monodispersed nanocluster beam. A major advantage of this type of system is that the clusters have much smaller size dispersion than grains obtained in any typical vapor deposition system. Studies with TEM and time-of-flight (TOF) mass spectrometer have shown that the observed lognormal size distribution has a standard deviation of about 10%. Applying a pulsed-field mass selector (Figure 1) to the nanocluster beam reduces this figure to about 3%. When oxygen gas is introduced into the deposition chamber during processing, uniform iron oxide shells covering the Fe clusters are formed. For a constant flow of Ar gas, the gas pressure in the deposition chamber can be adjusted by changing the flow rate of oxygen gas (O_2).

Fe nanoclusters of variable mean size of diameters from 2 to 100 nm are generated by the nanocluster source, which combines an improved high-pressure magnetron-sputtering gun with a gas-aggregation tube cooled by chilled water. We can control the cluster size by changing the flow rate of Ar gas (R_{Ar}), the flow rate of He gas (R_{He}), and the cluster growth length (L). One of the conditions to form a thick film of iron-iron oxide core-shell nanoclusters is to apply a power of 200 watts to the sputtering gun, when flow rate in the aggregation tube is 126 sccm of He and 564 sccm of Ar for about an hour. We are able to prepare about 5 mg/h of monodispersive nanoclusters for each size. For the preparation of Fe oxide-coated Fe clusters, we introduced oxygen gas at a flow rate around 4 sccm into the deposition chamber through a nozzle set behind the skimmer. Inside the deposition chamber, a chemical reaction began that formed iron oxide shells which covered the Fe clusters before they were deposited on the substrate. The clusters landed softly on the surface of substrates at room temperature and retain their original shape. This process ensures that all Fe clusters are uniformly oxidized before the cluster films are formed. We make a starch thin film on the surface of Si wafer, and then deposit the Fe clusters on the top of the starch film. The iron clusters can be easily dissolved and suspended in warm water for further bio-molecule conjugations. Detailed information about MNPs-molecule conjugation process will be published elsewhere.

Three kinds of substrates are used for the core-shell cluster deposition: transmission electron

microscopy (TEM) microgrids for HRTEM observations, silicon wafers for AFM and scanning electron microscopy (SEM) observations, and polyimide films for magnetic measurement. The effective film thickness of deposited clusters was estimated using a quartz crystal thickness monitor and the weight of the deposited cluster films was measured by a microbalance. Magnetic measurement was performed using a superconducting quantum interference device magnetometer (SQUID of MPMS XL-7) between 2 and 400 K with the maximum field of 70 kOe.

Results and discussion

Figure 2 shows a bright-field high-resolution SEM and AFM images of the core-shell Fe cluster assemblies deposited on the surface of a Si wafer. Using image-analysis software, we estimated the size distributions (inset of Figure 2) of the clusters recorded by a slow scan charge coupled device camera. In one example, as shown here, the mean cluster diameter (D) is 10.1 nm. The standard deviation is less than 10%. The distribution fits well to a lognormal function with a very narrow size distribution (Qiang, 1998, 2000, 2002, 2004; Meldrim, 2000; Sellmyer 2002; Xu, 2003).Our results clearly demonstrate that monodispersive nanoclusters in the size range of around 2–100 nm are reproducible by choosing the appropriate growth parameters R_{Ar}, R_{he}, and L.

Figure 3 shows high-resolution TEM (HRTEM) overviews of 4 single core-shell structured nanoclusters with size range from 3 to 85 nm deposited on a carbon film of microgrids. The nanoparticles appear almost spherical, and those that have a crystal axis oriented along the electron beam direction show two contrasts, a dark iron core region and a light-gray oxide shell. The electron diffraction pattern (Figure 4) obtained from a large sample area tells us the core has the bulk iron bcc lattice structure with the lattice fringe 0.286 nm. The HRTEM results also indicate that the oxide-coated Fe nanoclusters were covered uniformly with the Fe_3O_4 and/or Fe_2O_3 shells composed of very small nanocrystallites (Figure 5).

The iron oxide shell has a thickness of about 2.5 nm independent of the nanoparticle size. We observed that the core-shell nanoclusters are very stable against further oxidation after a long time exposure to air. According to our HRTEM measurements the shell thickness remains no change after the nanoclusters exposure to air more than 6 months. When we annealed the samples at 250°C for 3 h in the air, the shell thickness has increased to about 5 nm with slightly decreasing of the core size but the core-shell nanostructures remain intact. For sizes smaller than 7 nm, there are no core-shell structures (Figure 3a) because the oxidation goes through the entire nanoparticle.

Figure 6 shows hysteresis loops of Fe oxide-coated nanoclusters at room temperature. The samples with cluster size less than 15 nm are

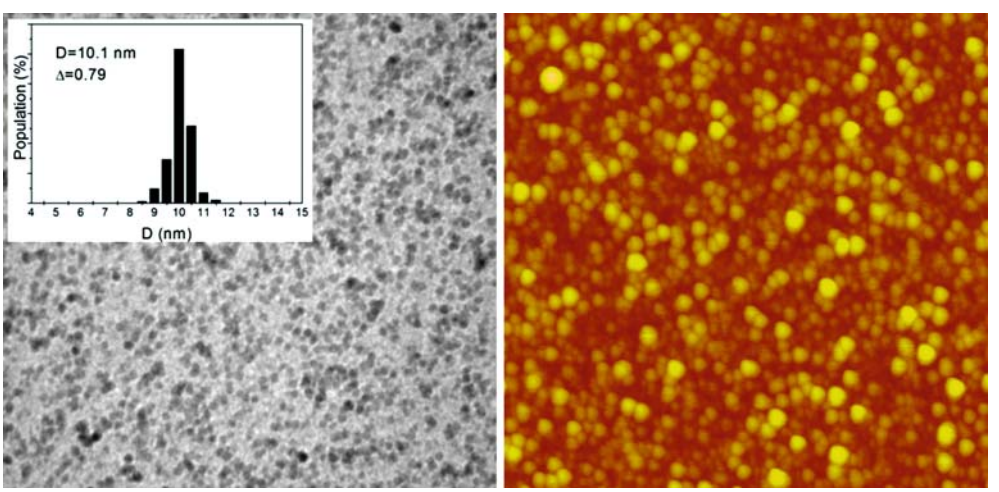

Figure 2. BF-TEM and AFM image and size distribution of iron/iron oxide clusters.

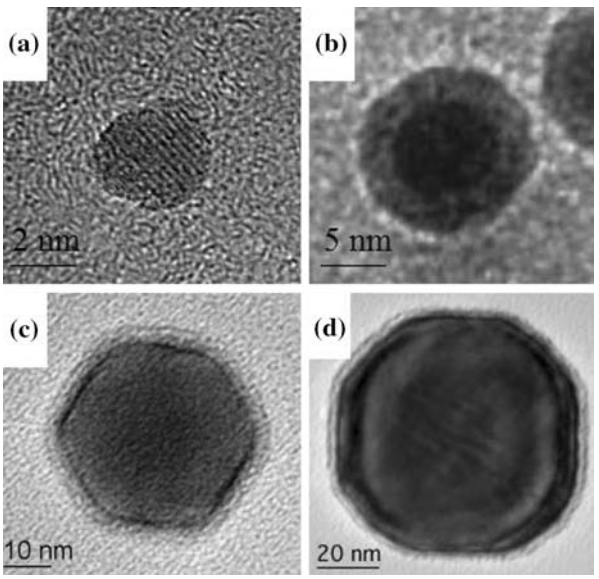

Figure 3. HRTEM micrographs of the oxide-coated Fe clusters with diameter from around 3 to 85 nm prepared on carbon microgrids.

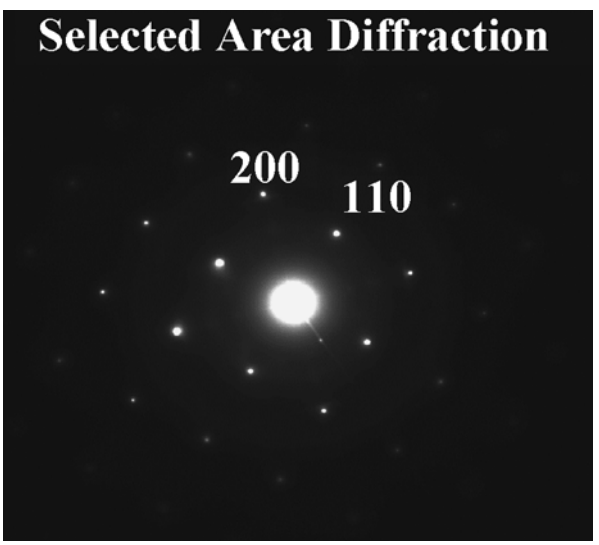

Figure 4. E-beam diffraction pattern on the core of clusters, which shows Fe BCC structure.

superparamagnetic at room temperature without coercivity. Figure 6a is one example of a cluster size of 10 nm. The field-cooling and zero-field-cooling measurements tell us the block temperature is about 45 K. The temperature increases as increasing of the nanocluster size. It is clear that this cluster exhibits superparamagnetic behavior. When the sizes of clusters are larger than 15 nm, they are ferromagnetic. The coercivity increases from 25 Oe for 15 nm size clusters to about 1 kOe for 100 nm clusters. Figure 6b shows a typical hysteresis loop of 85 nm diameter clusters with $H_c = 890$ Oe. Even at 4 T, the hysteresis loop has not been saturated due to many very small iron oxide nano-crystallites

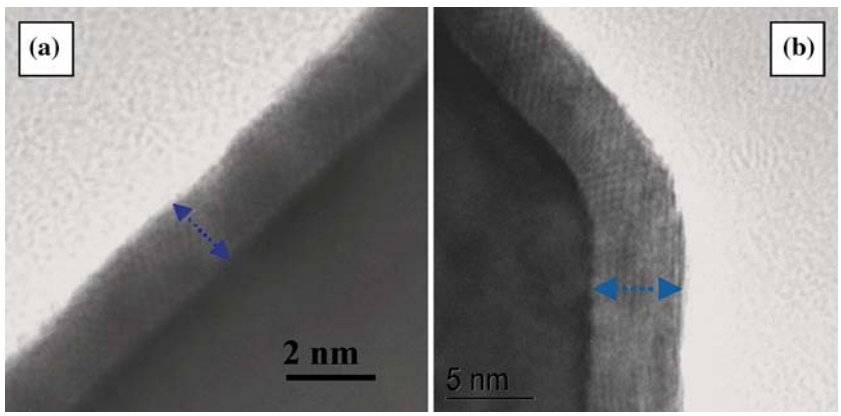

Figure 5. (a) The shell thickness is about 2.5 nm as deposited clusters, (b) the shell thickness increases to about 5 nm after annealing at 250°C for 3 h in the air.

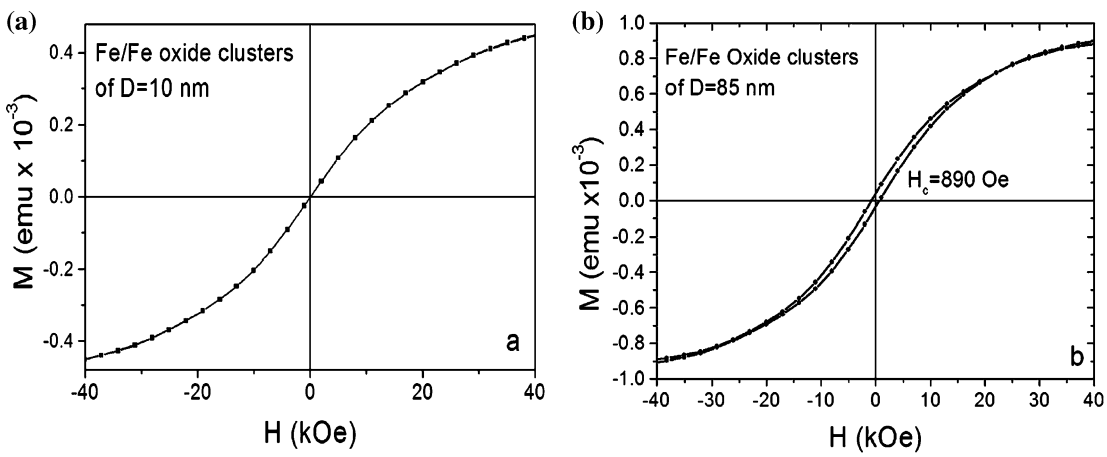

Figure 6. Hysteresis loops of iron oxide-coated Fe clusters with (a) $D = 10$ nm and (b) $D = 85$ nm at room temperature.

in the uniform shells, indicated in Figure 5. Those nano-crystallites are superparamagnetic at room temperature. All the samples at low temperature (4 K) are magnetically ordered with hysteresis loops and H_c is from 0.4 to 1.5 kOe as cluster sizes increase. We obtain the saturated magnetization (M_s) by a high-field fit to the expression $M = M_s(1-A/H^2)$, where A is a constant and H is the applied field. The results of M_s divided by the weight of the cluster films provide the specific magnetic moments with a unit of emu/g.

Figure 7 shows a curve of the specific magnetic moment versus the nanocluster size. It can be seen that it increases as cluster size increases from 3 to 100 nm. When the size is less than 10 nm, the specific magnetic moment is around 80 emu/g, similar to the value of ferromagnetic iron oxides – magnetite (Fe_3O_4). This information is consistent with the HRTEM image (Figure 3a), which shows that the entire nanocluster is oxidized to form a superparamagnetic iron oxide nanoparticle. If the cluster size is larger than 10 nm, the value of the specific magnetic moment increases dramatically until the cluster size reaches 100 nm where it almost saturates at 205 emu/g. This is close to the pure bulk Fe value (218 emu/g at room temperature). This value is almost 10 times larger than the value (20–30 emu/g) for iron oxide nanoparticles currently used in biomedical applications.

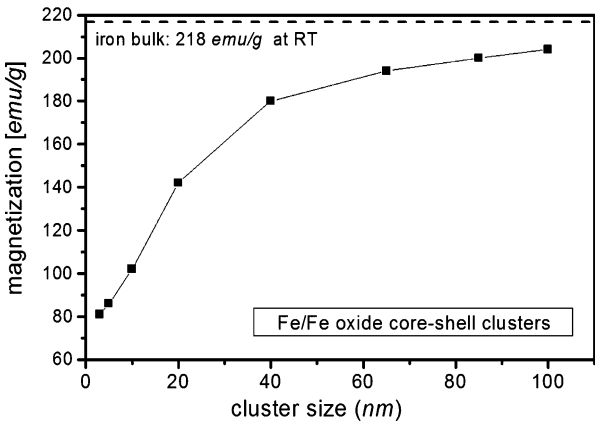

Figure 7. Size dependent specific magnetic moments of iron oxide-coated Fe nanoclusters.

Conclusion

In summary, monodispersive core-shell nanostructured clusters with high specific magnetic moments (about 200 emu/g) are synthesized by a new approach of the nanocluster deposition system. The size of core-shell nanoclusters can be changed easily from 2 to 100 nm by controlling the growth parameters. HRTEM images show the coatings are iron oxides which very uniformly cover the Fe cores. The nanoclusters of size less than 15 nm are superparamagnetic at room temperature and become ferromagnetic with increasing size. The specific magnetic moment of core-shell nanoclusters is size dependent, and increases rapidly from about 80 emu/g at the cluster size of around 3 nm to over 200 emu/g at the size of 100 nm. The use of high magnetic moment nanoclusters for biomedical applications could dramatically enhance the contrast for MRI, reduce the concentration of magnetic particle needs for cell separation, or make drug delivery possible with much lower magnetic field gradients.

Acknowledgements

Financial support from the NSF-EPSCoR, NIH-INBRE and the University Research Office of the University of Idaho for the purchase of a SQUID instrument (MPMS XL-7, Quantum Design, Ins) is gratefully acknowledged. TEM data was collected at EMSL, a user facility sponsored by the DOE and operated by Battelle. Dr. Chongmin Wang at PNNL is thanked for highly valuable TEM assistance.

References

Andra W. & H. Nowak,. 1998. Magnetism in Medicine. Berlin: Wiley-VCH.

Brigger I., C. Dubernet & P. Couvreur, 2002. Nanoparticles in cancer therapy and diagnosis. Adv. Drug Delivery Rev. 54631–54651.

Whitesides G. & A.P. Alivisatos, 1999. Fundamental scientific issues for nanotechnology Nanotechnology Research Directions. A.P. Alivisatos et al. ed. IWGN Workshop Report.

Cancer Nanotechnology Plan, A strategic Initiative to Transform Clinical Oncology and Basic Research through the Directed Application of Nanotechnology, U.S. Department of Health and Human Services, National Institutes of Health, National Cancer Institute, July 2004.

Fritzsche W. & T.A. Taton, 2003. Metal nanoparticles as labels for heterogeneous, chip-based DNA detection, Nanotechnology 14, R63–R73.

Hadjipanayis G.C., Siegel R.W. (eds.). 1994. Nanophase Materials. Dordrecht: Kluwer.

Haefeli U., Schuett W., Teller J., Zborowski M. (eds.). 1997. Scientific and Clinical Applications of Magnetic Carriers. New York: Plenum Press.

Hatch G.P. & R.E. Stelter, 2001. Magnetic design considerations for devices and particles used for biological high-gradient magnetic separation systems, J. Magn. Magn. Mater. 225, 262–276.

Jordan A., R. Scholz, K. Maier-Hauff, M. Johannsen, P. Wust, J. Nadobny, H. Schirra, H. Schmidt, S. Deger, S. Loening, W. Lanksch & R. Felix, 2001. J. Magn. Magn. Mater. 225, 118.

Kim Do K., M. Mikhaylova, Y. Zhang & M. Muhammed, 2003. Protective coating of superparamagnetic iron oxide nanoparticles, Chem. Mater. 15, 1617–1627.

Matijevic E. ed. 1989. Fine Particles A special issue in MRS Bulletin 14, 18; Matijevic E. 1993. Chem. Mater. 5, 412.

Meldrim J.M., Y. Qiang, D.J. Sellmyer & H. Haberland, 2000. Magnetic properties of cluster-beam synthesized Co-noble metal films, J. Appl. Phys. 87, 9–7013.

Portet D., B. Denizot, E. Rump, J.J. Lejeune & P. Jallet, 2001. J. Colloid Interface Sci. 238, 37.

Qiang Y., Y. Thurner, Th. Reiners, O. Rattunde & H. Haberland, 1998. TiN and TiAlN coatings deposited at room temperature by Energetic Cluster Impact (ECI), Surface and Coatings Technology 101/1–3, 27–32.

Qiang Y.R. Morel, E. Eastham, J.M. Meldrim, J. Kraft, A. Fert, H. Haberland & D.J. Sellmyer, 2000. Magnetic properties of cobalt clusters embedded in a nonmagnetic matrix (Ag, Cu, SiO_2), Cluster and Nanostructure Interfaces, Jena, P., Khanna, S.N. and Rao, B.K. eds. Would Scientific.

Qiang Y.R.F. Sabiryanov, S.S. Jaswal, Y. Liu, H. Haberland & D.J. Sellmyer, 2002. Magnetism of Co nanocluster films, Phys. Rev. B 66, 064404.

Qiang Y.J. Antony, M.G. Marino & S. Pendyala, 2004. Synthesis of core-shell nanoclusters with high magnetic moment for biomedical applications. IEEE Trans. Magnet. November 2004, 3538–3540.

Reich D.H., et al., 2003. Biological applications of multifunctional magnetic nanowires, J. Appl. Phys. 93, 7275–7280.

Sellmyer D.J., C.P. Lou, Y. Qiang & J.P. Liu, 2002. Magnetism of Nanophase composite films. In: Nalwa H.S. ed. Handbook of Thin Film Materials. 5 Academic Press, New York.

Sugimoto T., 2000. Fine Particles: Synthesis, Characterization and Mechanism of Growth. New York: Marcel Dekker.

Tada M.S., H. Hatanaka, N. Sanbonsugi, Matsushita & M. Abe, 2003. Method for synthesizing ferrite nanoparticles ~30 nm in diameter on neutral pH condition for biomedical applications, J. Appl. Phys. 93, 7566–7568.

Xu Y., Z. Sun, Y. Qiang & D. Sellmyer, 2003. Magnetic properties of L10-FePt and FePt:Ag nanocluster films, J. Appl. Phys. 93, 10–8289.

Zhao M., M.F. Kircher, L. Josephson & R. Weissleder, 2002. Differential conjugation of Tat peptide to superparamagnetic nanoparticles and its effect on cellular uptake, Bioconjug. Chem. 13, 840–844.